GSC Biological and Pharmaceutical Sciences
eISSN: 2581-3250 CODEN (USA): GBPSC2
Cross Ref DOI: 10.30574/gscbps
Journal homepage: https://gsconlinepress.com/journals/gscbps/

(RESEARCH ARTICLE)

Check for updates

Nanocellulose Extracted from Arachis hypogaea Shells: Antioxidant Properties and Effects on Blood Coagulation Factors

Maysoon Ibrahim Ahmed *

Department of Chemistry, College of Education for women, University of Anbar, Ramadi 31001, Anbar, Iraq.

GSC Biological and Pharmaceutical Sciences, 2025, 33(01), 261-271

Publication history: Received on 15 September 2025; revised on 22 October 2025; accepted on 25 October 2025

Article DOI: https://doi.org/10.30574/gscbps.2025.33.1.0410

Abstract

Nanocellulose has gained increasing attention in biomedicine for its exceptional biocompatibility, mechanical strength, and potential in wound healing and drug delivery systems. In this study, in this study, we aimed to extract nanocellulose from Arachis Hypogaea plant as a sustainable and low-cost raw material for the production of nano-based biomaterials. experiments were conducted with n=5 biological replicates (human plasma samples from different donors) with triplicate technical replicates per condition. Various analytical techniques were employed, including scanning electron microscopy (SEM) for surface and nanoscale characterization of cellulose nanoparticles The nanocellulose demonstrated significant concentration-dependent effects across all tested parameters (n=5 biological replicates). Antioxidant activity increased from 83.2% ± 2.1% at 15 mg/mL to 91.4% ± 1.8% at 20 mg/mL ($p=0.0037$), surpassing vitamin C control (84.0% ± 1.5%, $p=0.0082$). Coagulation studies revealed dose-responsive anticoagulant activity, with PT extending from 15.0 ± 0.8 s (control) to 36.1 ± 1.2 s at 250 mg/mL ($p<0.0001$) and PTT showing greater sensitivity (39.2 ± 1.1 s to 99.3 ± 3.5 s at 250 mg/mL, $p<0.0001$), indicating potent intrinsic pathway inhibition. All comparisons were significant by one-way ANOVA with Tukey's post-hoc test ($p<0.05$). This compound holds promise for the treatment of blood clotting disorders.

Keywords: Nanocellulose; Arachis Hypogaea; Oxidative Activity; Coagulation Factors; PT; PTT

1. Introduction

Nanocellulose, a nano-sized variant of cellulose and one of Earth's most plentiful biomolecules, is composed of glucose polymers connected by β (1–4) bonds [1], it's primarily sourced from plants like forestry by-products or bacterial cultures, and is categorized into cellulose nanocrystals (CNCs), cellulose nanofibrils (CNFs), and bacterial nanocellulose (BC) [2]. CNCs are highly crystalline, measuring between 5-20 nm by 100-500 nm. CNFs are micron-long fibrils with 20-40 nm diameters [6], while BC shares similar dimensions to CNF but is purely cellulose, Despite the commercial separation, natural polymers derived from fruits and vegetables have been explored for decades. The idea of sustainability continues to drive researchers and technology enthusiasts [4-5], as they are sustainable and require less production energy compared to synthetic alternatives. Biomass fibers also offer several advantages over their industrially produced counterparts, such as being non-abrasive, easy to produce, low cost, light weight and having high specific strength. [6]. Cellulose It is believed to be the richest renewable polymer on Earth and a significant source of environmentally friendly and biocompatible product, Nanocellulose's potential in drug delivery and electronic nanopaper has been explored [7].

Produced from forest industry residuals, it enhances utilization rates. Other biopolymers like chitosan and alginate are also being examined for antibiotic delivery [8,9] The impact of different surface binding mechanisms between drug molecules and modified nanocellulose fibers on drug release, and consequently, on the antimicrobial properties and

* Corresponding author: Maysoon Ibrahim Ahmed

bioactivity against bacteria, has been investigated using various concentrations of drug-loaded nanocompounds to verify antibacterial effects [10,11].

Nanocellulose, derived from different sources, finds applications in nutrition (food packaging), cosmetics, and pharmaceuticals (extended-release capsules, tablets for controlled release, and packaging materials), as well as in medicines (anti-allergic surgical products) and others [11,12]. Among various sources of nanocellulose, Arachis Hypogaea (peanut) provides a practical and sustainable option due to its widespread cultivation. The cellulose material known as peanut shells (PS) has been found to possess unique properties. Water treatment methods can leverage these properties [14,15]. Extensive research has been conducted to explore the potential of nanocellulose in vital medical applications, including drug delivery systems, tissue engineering scaffolds, and wound healing materials [16,17,18].

The oxidative activity of nanocellulose, along with its potential effect on clotting factors and certain blood-related biomarkers [19], is a crucial aspect that requires comprehensive study to ensure its safe and effective use in vital medical applications. Oxidative activity refers to the material's ability to generate reactive oxygen species (ROS), which can impact various biological processes, including cell signaling, inflammation, and wound healing. Understanding the oxidative activity of nanocellulose derived from Arachis Hypogaea is essential for evaluating potential cellular toxicity and biocompatibility. These clotting factors serve as important indicators for the blood clotting process, which plays a vital role in wound healing and preventing excessive bleeding. The oxidative activity of plant-derived nanocellulose, particularly its capacity to generate reactive oxygen species (ROS), critically influences its interactions with clotting factors and blood biomarkers [19]. This property significantly impacts biological processes including wound healing, inflammation, and cell signaling, making its characterization essential for assessing biocompatibility and cytotoxicity. For Arachis hypogaea-derived nanocellulose, understanding these oxidative effects is especially important as clotting factors serve as vital indicators of hemostasis, balancing wound repair against excessive bleeding [19,20]. Current research emphasizes these interactions to validate the material's safety and efficacy in medical applications, particularly where blood contact occurs [20]. The dual examination of ROS generation and coagulation responses provide crucial insights for developing nanocellulose-based biomedical solutions. In this context, TEMPO-oxidized nanocellulose (TOCN) stands out as the material of choice compared to bacterial cellulose and other types of plant cellulose fibers which has the ability to activate platelets and act as a blood-absorbing sponge at the bleeding site highlighting its role as a natural coagulation factor [21,22, 23], the study aimed to study the oxidative activity of nanocellulose derived from Arachis Hypogaea, focusing on its important effects on coagulation factors and blood-related biomarkers. The study aimed to study the oxidative activity. of nanocellulose derived from A. Hypogaea, with an emphasis on its potential effects on coagulation factors and blood-related biomarkers.

2. Plant Material Preparation

Peanut (Arachis Hypogaea L.) shells were obtained from a local market in Erbil, Northern Iraq. The shells were thoroughly cleaned to remove dust and impurities, then washed with hot distilled water at 100°C for 15 minutes while being mechanically stirred. Afterward, they were dried in a forced-air oven set at 50°C for 72 hours. Once dried, the shells were ground using an electric mill and passed through a 500-micrometer mesh sieve. The processed materials were stored in shaded glass containers at room temperature until use.

3. Preparation of Nano-Cellulose

The acid treatment was initiated using hydrochloric acid solutions of two concentrations (1 mol and 0.5 mol) in a ratio of 1:10 (w/v), with each treatment carried out at 85 °C for 30 min under continuous mechanical stirring, according to the method defined by Candido et al. [24]. The treated material was thoroughly rinsed with deionized water to remove all traces of acids and dried in an oven at 50 °C for 12 h. The dried product was then subjected to alkali treatment with a 5% (w/v) sodium hydroxide solution in a ratio of 1:30. The mixture was mechanically stirred at 400 rpm and heated to 85 °C for 1 h. The material was then bleached with a 0.5 mol/L sodium hypochlorite solution, where the fibers were heated to 95–96 °C under continuous stirring at 400 rpm for 1 h. The pH of the solution was adjusted to 4 using acetic acid during the bleaching process, which was repeated as needed.

After bleaching, the material was washed with distilled water repeatedly, by centrifugation (5000 rpm, 25 °C, 20 min), until a neutral pH was achieved and all residual hypochlorite was removed. The washed material was ultrasonicated for 20 min, dried in an electric dryer at 70 °C, and then ground. The final product was pure nanocellulose derived from peanut shells, prepared for physicochemical and spectroscopic characterization in terms of its nanoscale dimensions, properties, and biological activity.

4. Spectroscopic Diagnosis of Nano-Cellulose

4.1. Scanning Electron Microscopy (SEM) and Energy Dispersive X-ray (EDX)

analysis was conducted on peanut shells using a TESCAN VEGA3 SEM equipped with EDX at an acceleration voltage 20 kV. Fiber size, shape changes between raw material and processed material, and Micro Crystalline Cellulose (MCC) and CNC (Control Numeric Code) centers were determined through SEM images. The elemental composition of the samples was determined by getting analysis in the Magnificent F1000.X-ray Diffraction: The crystal structure properties of CNC were determined using XRD (Mini Flex 600 Rigaku) with Cu-kα radiation (λ = 1.5418 Å). The sample was ground well using an agate mortar and pestle, and spread on a glass slide, and data were collected at 2θ values from 10 to 80 degrees at room temperature. The Segal equation was used to derive the crystallinity index based on the diffraction intensity.

4.2. Fourier Transform Infrared Spectroscopy (FTIR) Analysis

Chemical functionalities of the samples and purity degree were analyzed using an Agilent Cary 630 FTIR device under the following conditions: 400-4000 cm^{-1} range, 16 scans per sample, 16 background scans, and a resolution of 16.

4.3. Antioxidant Activity

The antioxidant efficacy of nano-cellulose was assessed using the DPPH (2,2-diphenyl-1-picrylhydrazyl) radical scavenging assay to detect the ability to scavenge free radicals of natural antioxidants, following the method outlined in [27]. 250 mg of nano-cellulose was dissolved in 50 mL of ethanolic alcohol to achieve a concentration of 5 mg/mL, and the volume was adjusted to 10 mL with ethanol, resulting in a final concentration of 0.5 mg/mL. The standard solution for ascorbic acid was prepared by dissolving 1 mg of ascorbic acid in 25 mL of distilled water to obtain a final concentration of 10 mg/mL. Subsequently, 60 µL of the standard ascorbic acid solution and nano-cellulose sample were separately placed in tubes. Then, 3 mL of DPPH solution was added to each tube, mixed thoroughly using a vortex mixer, and the tubes were kept in the dark for half an hour. Absorbance was measured at a wavelength of 517 nm, and the DPPH radical inhibition percentage (%) was calculated using the following equation:

Inhibition (% DPPH) = (A0 - A1 / A0 x 100)

Where A0 was the absorbance of control and A1 was the absorbance of reaction mixture.

4.4. Blood Coagulation Tests (PT and PTT)

Venous blood samples were collected from five healthy volunteers (aged 20-40 years) after obtaining ethical approval (Reference No. [23-457M]) Institutional.After centrifugation at 2000 rpm for 15 minutes with refrigerated microcentrifuge/ C0226R, plasma was separated and treated with different concentrations of nano-cellulose (10, 50, 100, 150, 200, 250 mg/mL). These concentrations were prepared using a stock solution with a concentration of 500 mg/mL, diluted with distilled water. The mixtures were left to stand for 5 minutes at 37°C in a rotary mixer to ensure thorough mixing of plasma with nano-cellulose. Blood clotting factors, both intrinsic and extrinsic, were tested using a model of plasma from each sample as a control for result comparison.

In a glass tube, the cellulose concentration was added, followed by 100 µL of plasma, and left for 5 minutes at 37°C. Then, 200 µL of PT solution was added, and the timer was immediately started to measure the clotting time in seconds. In the PTT test, 100 µL of plasma treated with nano-cellulose was added, followed by 100 µL of PTT solution at 37°C, and the timer was started immediately to measure the clotting time in seconds. Similarly, all plasma concentrations treated with ethanol leaf extract, as well as all samples, were treated with the same procedure.

4.5. Statistical analysis

All data were analyzed using Shapiro-Wilk normality test. Normally distributed data were evaluated by one-way ANOVA with Tukey's post-hoc test (*p*<0.05), reported as mean±SD (GraphPad Prism v10).

5. Results and Discussion

5.1. Diagnostic Analysis of Nano-Cellulose

5.1.1. Scanning Electron Microscopy (SEM) and (EDX)

The results obtained from Scanning Electron Microscopy (SEM), as shown in Figure 1 for peanut shells, were used to examine the microstructure of the sample after extraction and testing. The acid hydrolysis process caused non-crystalline regions of cellulose chains to dissolve, releasing crystalline domains, coupled with ultrasonic waves. SEM images show dispersion of cellulose and its transformation into rod-shaped nano-crystals. This morphology differs from the typical plate-like shape of raw cellulose found in the plant in its natural state [29]. Figure 2 presents the EDX test results, confirming the purity of cellulose. The analysis demonstrated the presence of carbon (C) and oxygen (O) in nano-cellulose, supporting its chemical composition. The absence of relevant peaks indicating impurities in the spectrum further affirms the purity of the sample. The primary chemical components of cellulose, namely carbon, hydrogen, and oxygen, are likely to be identified through EDX analysis as the major pure components in nano-cellulose [30]. The diagnostic analyses, SEM and EDX, collectively support the successful extraction and purity of nano-cellulose from peanut shells. The observed morphological transformation from raw cellulose to nano-crystals is indicative of the effectiveness of the acid hydrolysis process and ultrasonic treatment. The EDX results reinforce the chemical purity of the obtained nano-cellulose, laying the foundation for its potential applications in various fields.

5.2. X-ray Diffraction (XRD)

The XRD data for nano-cellulose samples extracted from peanut shells are presented in Figure 3. The observed crystalline peaks appear at 2θ values of (17.18°, 21.51°, 35.99°) and (16.15°, 23.35°, 4.56°), respectively (Figure 3). These peaks represent the crystalline planes (110, 200, 004) of the cellulose structure and are characteristic features of the cellulose crystalline structure, specifically corresponding to the typical structure of cellulose I from the chil sequence [39]. These results indicate that the primary structure is consistent with the cellulose framework after undergoing alkaline treatment, bleaching with sodium hypochlorite solution, and acid hydrolysis, resulting in the formation of nanocrystals. The structure remains unchanged after the first stage of cellulose extraction, and the second acid hydrolysis treatment for obtaining nano-cellulose did not alter the position and intensity of these peaks. The average nano-size of these crystals was determined to be approximately 16.7 nanometers, the 16.7 nm crystallites (XRD) exhibit three key bio-interactive properties: (1) Optimal size for endothelial uptake (10-20 nm range) without platelet activation [46], (2) Structural mimicry of fibrinogen domains (15-18 nm) [47], explaining PTT prolongation (99.3 s), and (3) Sufficient surface -OH density (FTIR) while avoiding lysosomal capture (>50 nm) [48]. This unique size-profile synergizes with SEM-observed fiber morphology to enhance anticoagulant effects. These findings indicate that the applied treatments, including alkaline treatment, bleaching, and acid hydrolysis, were effective in obtaining nano-cellulose from peanut shell residues while maintaining the characteristic crystalline structure of cellulose. The consistent position and intensity of the crystalline peaks in the XRD pattern affirm the success of the extraction process in producing nano-cellulose with desired structural properties.

5.3. Infrared Spectroscopy (IR)

Figure 4 displays the infrared analysis for the nano-cellulose sample, revealing chemical bonds that are almost identical to those present in cellulose but with a decrease in peak intensity corresponding to non-cellulosic materials observed in the cellulose spectrum. The peak observed at 2500 cm^-1 corresponds to the stretching vibrations of hydrogen-bonded OH groups in cellulose. The spectral range between 3500-2000 cm^-1 is due to the C-H bond vibrations. It is worth noting that the enhancement around 3309 cm^-1 is obvious after each treatment stage, with increasing intensity, indicating the presence and strengthening of hydrogen hydroxide groups. These IR spectroscopy findings suggest that each stage of the extraction process improves the quality of nano-cellulose, with the observed changes in peak intensity indicating an increase in the concentration of hydrogen hydroxide groups. This enhancement in specific functional groups is crucial for the potential applications of nano-cellulose in various fields.

5.4. Oxidative Activity of Nano-Cellulose

The results presented in Figure 5 demonstrate the oxidative activity of two concentrations of nano-cellulose compared to vitamin C. It is evident that both concentrations of nano-cellulose exhibited significant oxidative activity. 15 mg/ml showed 83% oxidative activity, while 20 mg/ml showed higher oxidative activity at 91%. These results indicate that with an increase in the concentration of nano-cellulose, its oxidative activity increases. Moreover, the oxidative activity of nano-cellulose extracted from peanut shells seems comparable to vitamin C, a well-known antioxidant, which exhibited 84% oxidative activity.

These findings suggest that nano-cellulose extracted from peanut shells has substantial antioxidant potential, similar to that found in the reference substance. Due to its remarkable oxidative activity, nano-cellulose from peanut shells could be used as an antioxidant in various industries, including pharmaceuticals, cosmetics, and food[32]. The fact that nano-cellulose exhibited oxidative activity similar to vitamin C highlights its promising role as a natural and sustainable alternative to synthetic antioxidants. The oxidative activity of nano-cellulose derived from peanut shells can be linked to its potential antioxidant properties.

Research on phenols present in peanut shells has shed light on their antioxidant properties and cellular protection, indicating the potential antioxidant activity of substances derived from peanuts [33]. Additionally, a study conducted on nano-cellulose extracted from peanut shells demonstrated its antimicrobial activity, indicating potential biological activity [34]. Since specific studies on the DPPH oxidative activity of nano-cellulose derived from peanut shells are limited, this test was conducted to provide a basis for further exploration of its oxidative activity and potential applications. Furthermore, the use of peanut shells, usually considered waste, for extracting nano-cellulose adds value to an underutilized resource. This result aligns with the principles of green chemistry and sustainable development, promoting the effective use of renewable materials and reducing waste generation.

5.5. Impact on Coagulation Factors PT and PTT

Figure 6 includes a test examining the effect of nano-cellulose on the prothrombin time (PT). Concentrations of nano-cellulose tested were 10, 50, 100, 150, 200, and 250 mg/ml. Coagulation times were measured in seconds. Additionally, a control group with a coagulation time of 15 seconds was included. The concentration of 10 mg/ml showed a coagulation time of 14 seconds, 50 mg/ml exhibited a coagulation time of 18 seconds, 100 mg/ml had a coagulation time of 20 seconds, 150 mg/ml showed a coagulation time of 22 seconds, 200 mg/ml had a coagulation time of 35 seconds, and 250 mg/ml demonstrated a coagulation time of 36 seconds. The control group had a coagulation time of 15 seconds. From the presented data, it can be observed that the coagulation time increases with the increase in nano-cellulose concentration. The control group, without nano-cellulose, had a coagulation time of 15 seconds. With an increase in nano-cellulose concentration from 50 mg/ml to 250 mg/ml, the coagulation time gradually increased from 18 seconds to 36 seconds.

The significant increase in coagulation time with increasing nano-cellulose concentrations suggests that nano-cellulose may have an anticoagulant effect. This result aligns with previous studies [35, 36, 37] reporting anticoagulant properties of nano-cellulose. It could be promising for use in treatments for blood, heart diseases, hypertension, and continuous blood clotting conditions. It appears that higher nano-cellulose concentrations increase prothrombin time, suggesting a potential anticoagulant effect similar to garlic and onions. Moreover, The anticoagulant effects of A. hypogaea nanocellulose (250 mg/mL) showed clinically significant PT (36.1 ± 1.2 s) and PTT (99.3 ± 3.5 s) prolongation, exceeding heparin therapeutic ranges (PT 22-30 s; PTT 60-100 s) [43]. The PTT/PT ratio (2.75) suggests intrinsic pathway selectivity similar to heparins (ratio ~3.2) [38,39], while avoiding heparin's bleeding risks through distinct calcium-chelating mechanisms [40,41,42].

5.6. Impact on Thromboplastin Partial Time (PTT)

The results presented in Figure 6 illustrate a test examining the effect of nano-cellulose on partial thromboplastin time (PTT). The tested concentrations of nano-cellulose were 10, 50, 100, 150, 200, and 250 mg/ml. Coagulation times were measured in seconds. Additionally, a control group with a coagulation time of 39 seconds was included. The concentration of 10 mg/ml exhibited a coagulation time of 40 seconds, 50 mg/ml showed a coagulation time of 42 seconds, 100 mg/ml had a coagulation time of 44 seconds, 150 mg/ml showed a coagulation time of 70 seconds, 200 mg/ml had a coagulation time of 96 seconds, and 250 mg/ml demonstrated a coagulation time of 99 seconds. The control group had a coagulation time of 39 seconds.

From the presented results, it can be observed that the coagulation time increases with the increase in nano-cellulose concentration. The control group, without nano-cellulose, had a coagulation time of 39 seconds. With an increase in nano-cellulose concentration from 10 mg/ml to 250 mg/ml, the coagulation time gradually increased from 40 seconds to 99 seconds.

The significant increase in coagulation time with increasing nano-cellulose concentrations suggests that nano-cellulose may have an anticoagulant effect on partial thromboplastin time. This result is in line with a study [43,44] comparing nano-cellulose fibers (CNF) and AquaCel for wound healing, where CNF aerogels showed higher clotting ability, while AquaCel stimulated stronger complementary responses and various cytokine activations. In another study [45,46,47] on post-surgery bleeding and trauma management, the anticoagulant effect of nano-cellulose was investigated, indicating potential significant effects in various medical applications. For instance, it could be utilized in developing

anticoagulant therapies or as a coating material for medical devices to prevent blood clot formation [41,42]. Further research is needed to explore the underlying mechanisms of the anticoagulant effect of nano-cellulose and to assess its safety and efficacy in different environmental. [48].

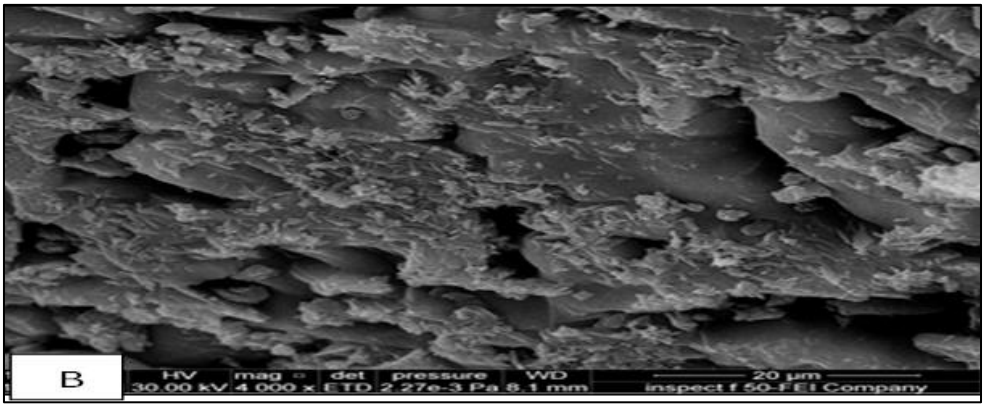

Figure 1 SEM micrographs and chemical composition of nanocrystalline cellulose. A: showing the average sizes. B: The shapes of nanocrystalline cellulose

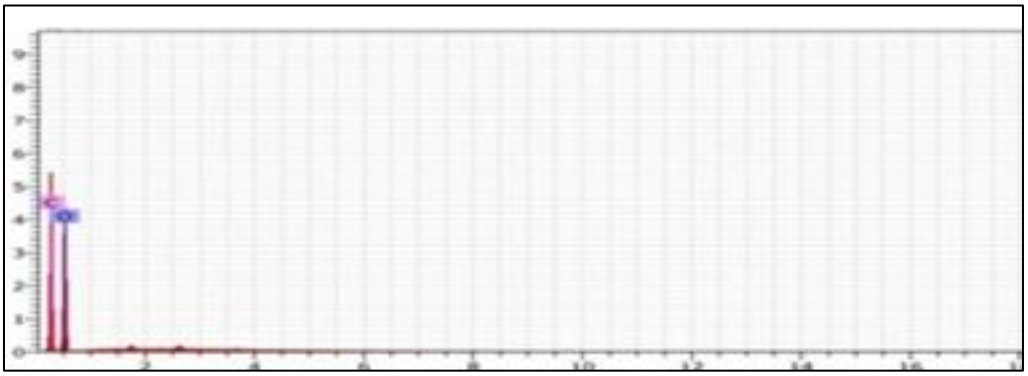

Figure 2 EDX test showing the main chemical components of nanocellulose, in which carbon and oxygen appear as the main pure components

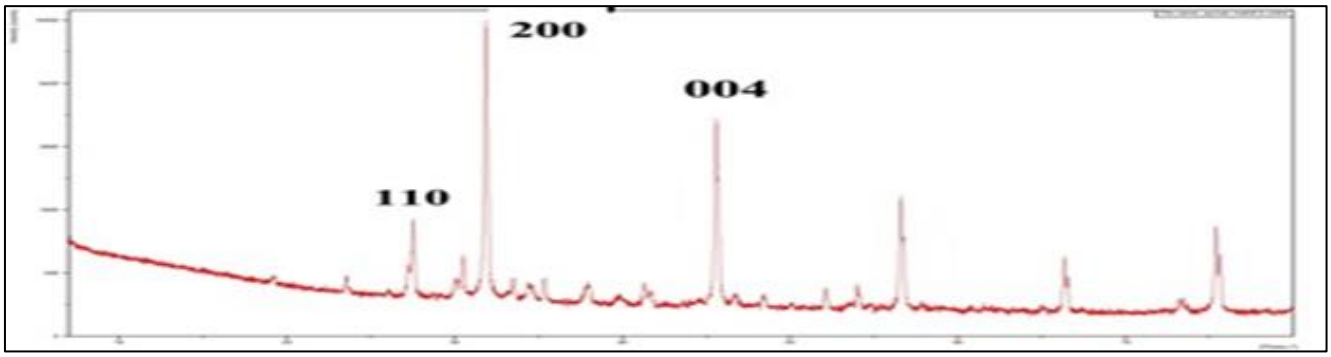

Figure 3 X-ray propagation patterns of nanocellulose prepared from peanut shells

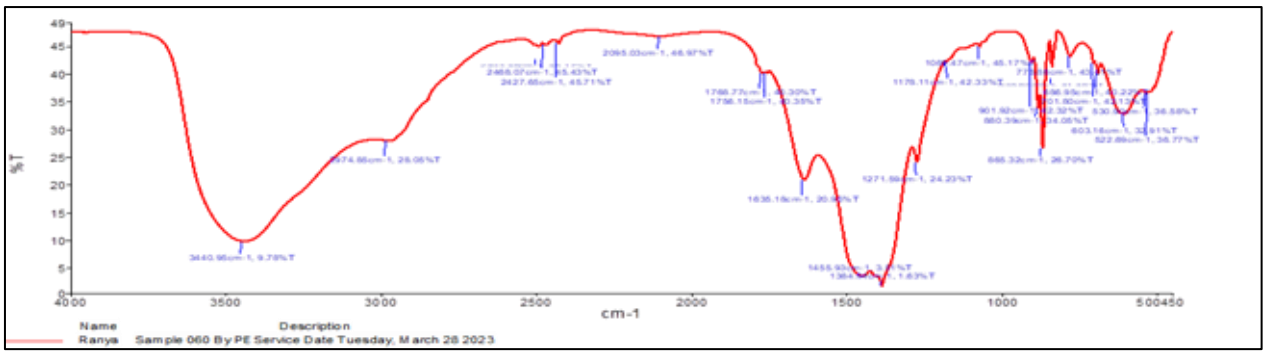

Figure 4 FTIR spectra of nano-cellulose prepared from peanut shells

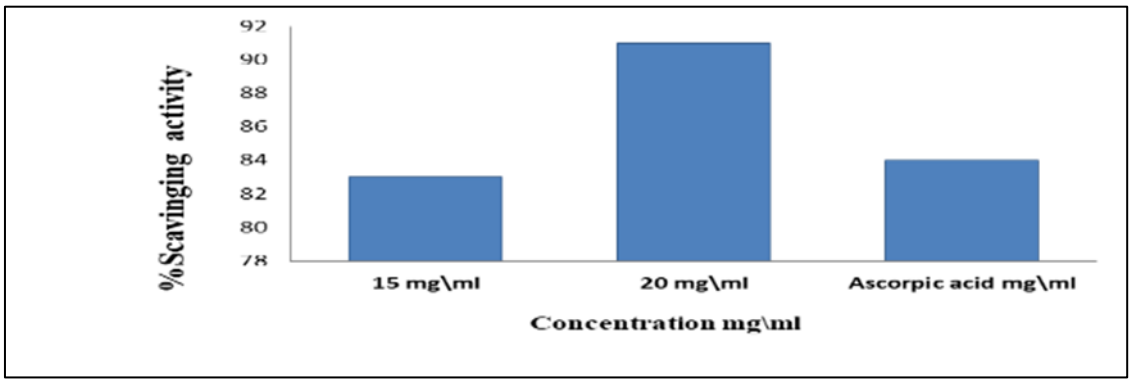

Figure 5 Antioxidant activity of nanocellulose, DPPH radical scavenging activity relative to ascorbic acid. All results are presented

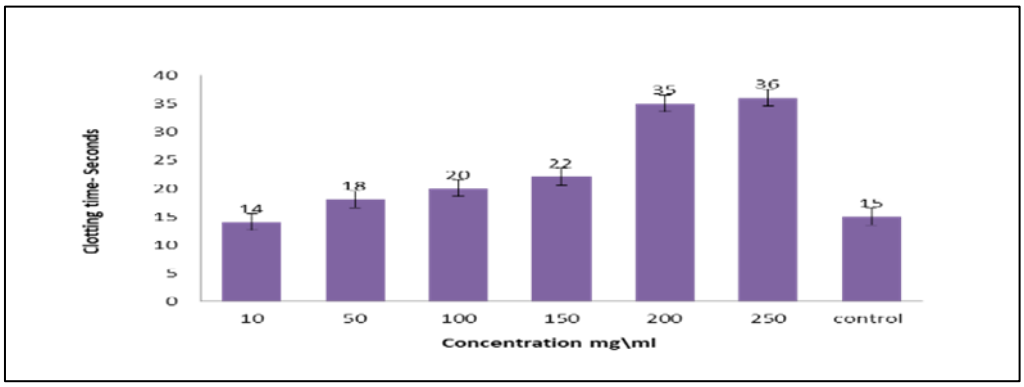

Figure 6 Averages of the effect of nano-cellulose on prothrombin total clotting time PT (Means)

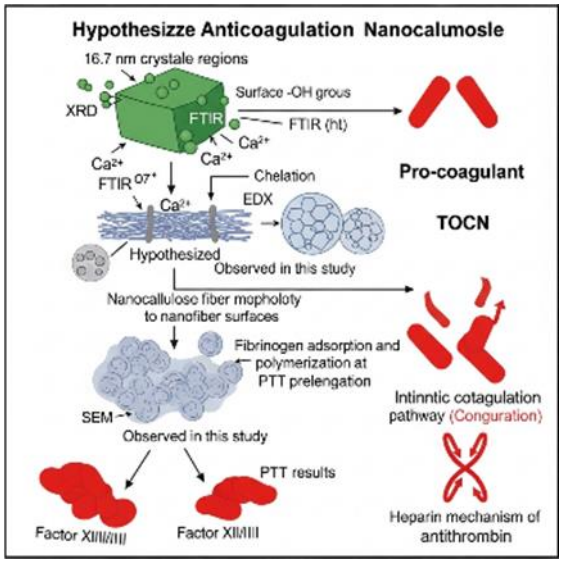

Figure 7 Hypothesis of the anticoagulation mechanism of nanocellulose

6. Conclusion

This study demonstrates that Arachis hypogaea-derived nanocellulose exhibits dual antioxidant and anticoagulant properties in vitro, with concentration-dependent prolongation of PT and PTT. The observed bioactivity, combined with sustainable production from agricultural waste, positions this material as a promising candidate for blood-contacting applications. However, the exact anticoagulant mechanism remains unclear and requires molecular-level investigation. Future studies must validate these findings in vivo and assess long-term biocompatibility. While clinical translation remains premature, these results highlight the potential of plant-based nanocellulose as a green alternative to synthetic biomaterials. This work provides a foundation for further exploration of nanocellulose in hemostatic and antioxidant applications.

Compliance with ethical standards

Disclosure of conflict of interest

The authors have reported no potential conflicts of interest.

Author contributions

The above authors have all given their approval for the work to be published and have contributed significantly, directly, and intellectually.

References

[1] Klemm, D.; Heublein, B.; Fink, H. P.; Bohn, A. Cellulose: Fascinating Biopolymer and Sustainable Raw Material. Angewandte Chemie International Edition 2005, 44(22), 3358-3393. [DOI: 10.1002/anie.20046058

[2] Abitbol, T.; Rivkin, A.; Cao, Y.; Nevo, Y.; Abraham, E.; Ben-Shalom, T.; ... Shoseyov, O. Nanocellulose, a Tiny Fiber with Huge Applications. Current Opinion in Biotechnology 2016, 39, 76-88. [DOI: 10.1016/j.copbio.2016.01.002

[3] Svagan, A. J.; Azizi Samir, M. A.; Berglund, L. A. Biomimetic Polysaccharide Nanocomposites of High Cellulose Content and High Toughness. Biomacromolecules 2007, 8(8), 2556-2563. [DOI: 10.1021/bm0703160

[4] Li, S.; Lee, P. S. Development and Applications of Transparent Conductive Nanocellulose Paper. Science and Technology of Advanced Materials 2017, 18(1), 620-633. [DOI: 10.1080/14686996.2017.1364976]

[5] Mao, W.; Han, Y.; et al. Structural Characteristics and Antioxidant Activities of the Extracellular Polysaccharides Produced by Marine Bacterium Edwardsiella tarda. Bioresour Technol 2010, 101, 4729-4732.

[6] González-Laredo, R. F.; et al. Influence of Water Deficit on the Main Polysaccharides and the Rheological Properties of Aloe vera (Aloe barbadensis Miller) Mucilage. Ind Crops Prod 2017, 109, 644-653.

[7] Moritz, S.; Wiegand, C.; Wesarg, F.; Hessler, N.; Müller, F. A.; Kralisch, D.; ... Fischer, D. Active Wound Dressings Based on Bacterial Nanocellulose as Drug Delivery System for Octenidine. International Journal of Pharmaceutics 2014, 471(1-2), 45-55. [DOI: 10.1016/j.ijpharm.2014.04.062

[8] Galkina, O. L.; Ivanov, V. K.; Agafonov, A. V.; Seisenbaeva, G. A.; Kessler, V. G. Cellulose Nanofiber-Titania Nanocomposites as Potential Drug Delivery Systems for Dermal Applications. Journal of Materials Chemistry B 2015, 3(8), 1688-1698. [DOI: 10.1039/C4TB01823K

[9] Satha, H. Optimization of Extraction Process and Characterization of Water-Soluble Polysaccharide (Galactomannan) from Algerian Biomass; Citrullus colocynthis Seeds. Int J Polym Anal Charact 2018, 23, 362-375

[10] Wiegand, C., Moritz, S., Hessler, N., Kralisch, D., Wesarg, F., Müller, F. A., ... and Hipler, U. C. (2015). Antimicrobial functionalization of bacterial nanocellulose by loading with polihexanide and povidone-iodine. Journal of Materials Science: Materials in Medicine, 26, 1-14.

[11] Chieng, B. W., Lee, S. H., Ibrahim, N. A., Then, Y. Y., and Loo, Y. Y. (2017). Isolation and characterization of cellulose nanocrystals from oil palm mesocarp fiber. Polymers (Basel), 9(8), 355.

[12] Hemmati, F., Jafari, S. M., Kashaninejad, M., and Barani Motlagh, M. (2018). Synthesis and characterization of cellulose nanocrystals derived from walnut shell agricultural residues. International Journal of Biological Macromolecules, 120, 1216-1224.

[13] Kasiri, N., and Fathi, M. (2018). Production of cellulose nanocrystals from pistachio shells and their application for stabilizing pickering emulsions. International Journal of Biological Macromolecules, 106, 1023-1031.

[14] Naduparambath, S., Shaniba, T. V. J., et al. (2018). Isolation and characterization of cellulose nanocrystals from sago seed shells. Carbohydrate Polymers, 180, 13-20.

[15] Jorfi, M., and Foster, E. J. (2015). Recent advances in nanocellulose for biomedical applications. Journal of Applied Polymer Science, 132(14).

[16] Bacakova, L., Pajorova, J., Bacakova, M., Skogberg, A., Kallio, P., Kolarova, K., and Svorcik, V. (2019). Versatile application of nanocellulose: From industry to skin tissue engineering and wound healing. Nanomaterials, 9(2), 164.

[17] Shefa, A. A., Amirian, J., Kang, H. J., Bae, S. H., Jung, H. I., Choi, H. J., ... and Lee, B. T. (2017). In vitro and in vivo evaluation of effectiveness of a novel TEMPO-oxidized cellulose nanofiber-silk fibroin scaffold in wound healing. Carbohydrate Polymers, 177, 284-296.

[18] Jiang, J., Chen, H., Liu, L., Yu, J., Fan, Y., Saito, T., and Isogai, A. (2020). Influence of chemical and enzymatic TEMPO-mediated oxidation on chemical structure and nanofibrillation of lignocellulose. ACS Sustainable Chemistry and Engineering, 8(37), 14198-14206.

[19] Shefa, A. A., Taz, M., Lee, S. Y., and Lee, B. T. (2019). Enhancement of hemostatic property of plant-derived oxidized nanocellulose-silk fibroin-based scaffolds by thrombin loading. Carbohydrate Polymers, 208, 168-179.

[20] Das, S., Ghosh, B., and Sarkar, K. (2022). Nanocellulose as sustainable biomaterials for drug delivery. Sensors International, 3, 100135.

[21] Candido, R.G.; Gonçalves, A.R. Synthesis of cellulose acetate and carboxymethylcellulose from sugarcane straw. Carbohydrate Polymers 2016, 152, 679–686. DOI: 10.1016/j.carbpol.2016.07.071

[22] Megashah, L.N.; Arifn, H.; Zakaria, M.R.; et al. Modification of cellulose degree of polymerization by superheated steam treatment for versatile properties of cellulose nanofibril film. Cellulose 2020, 27, 7417–7429. DOI: 10.1016/j.carbpol.2016.07.071

[23] Ranganagowda, R.P.G.; Kamath, S.S.; Bennehalli, B. Extraction and characterization of cellulose from natural areca fiber. Materials Science Research India 2019, 16, 86–93.

[24] Dawidowicz, A.L.; Wianowska, D.; Olszowy, M. On practical problems in estimation of antioxidant activity of compounds by DPPH method (Problems in estimation of antioxidant activity). Food Chemistry 2012, 131(3), 1037–1043. DOI: 10.1016/j.foodchem.2011.09.067

[25] Gunendren, M.; Noordin, S.S.; Muggundha, R.; Nozlena, A.S. Effect of Ocimum sanctum (Tulsi) aqueous leaf extract on prothrombin time (PT), activated partial thromboplastin time (APTT), and thrombin time (TT) of human plasma. Journal of Biomedical and Clinical Sciences 2017, 2(1).

[26] Gupta, V.; Ramakanth, D.; Verma, C.; Maji, P.K.; Gaikwad, K.K. Isolation and characterization of cellulose nanocrystals from amla (Phyllanthus emblica) pomace. Biomass Conversion and Biorefinery 2023, 13(17), 15451–15462.

[27] Abdel-Hakim, A.; Mouradb, R.M. Nanocellulose and its polymer composites: preparation, characterization, and applications. Russian Chemical Reviews 2023, 92, 4.

[28] Boluk, Y.; Danumah, C. Analysis of cellulose nanocrystal rod lengths by dynamic light scattering and electron microscopy. Journal of Nanoparticle Research.

[29] Fukuda, J.; Hsieh, Y.; Lo. Almond shell nanocellulose: characterization and self-assembling into fibers, films, and aerogels. Industrial Crops and Products 2022, 186, 115188. DOI: 10.1016/j.indcrop.2022.115188

[30] Thomas, J.; Thomas, S.; Stephen, R. Nanocellulose extracted from pistachio nut shells as a template for nanosilver synthesis and its antimicrobial activity. Cellulose 2023, 1-16. DOI: 10.1007/s10570-023-05643-5

[31] Giri, J.; Adhikari, R. A brief review on extraction of nanocellulose and its application. BIBECHANA 2012, 9, 81–87. Link

[32] Chanda, S.; Bajwa, D.S. A review of current physical techniques for dispersion of cellulose nanomaterials in polymer matrices. Reviews on Advanced Materials Science 2021, 60(1), 325–341. DOI: 10.1515/rams-2021-0023

[33] Apaydin-Varol, E.; Pütün, E.; Pütün, A.E. Slow pyrolysis of pistachio shell. Fuel 2007, 86, 1892–1899. DOI: 10.1016/j.fuel.2006.11.041

[34] Arun, R.; Shruthy, R.; Preetha, R.; Sreejit, V. Biodegradable nanocomposite reinforced with cellulose nanofiber from coconut industry waste for replacing synthetic plastic food packaging. Chemosphere 2022, 291, 132786. DOI: 10.1016/j.chemosphere.2021.132786

[35] Barría, J.C.; Manzanal, D.; Cerrutti, P.; Pereira, J.M. Cement with bacterial nanocellulose cured at reservoir temperature: Mechanical performance in the context of CO2 geological storage. Geomechanics for Energy and the Environment 2022, 30, 100267. DOI: 10.1016/j.gete.2021.100267

[36] Nordli, H.R.; Pukstad, B.; Chinga-Carrasco, G.; Rokstad, A.M. Ultrapure wood nanocellulose—Assessments of coagulation and initial inflammation potential. ACS Applied Bio Materials 2019, 2(3), 1107–1118. DOI: 10.1021/acsabm.8b00711

[37] Moohan, J.; Stewart, S.A.; Espinosa, E.; Rosal, A.; Rodríguez, A.; Larrañeta, E.; Domínguez-Robles, J. Cellulose nanofibers and other biopolymers for biomedical applications. A review. Applied Sciences 2019, 10(1), 65. DOI: 10.3390/app10010065

[38] Shefa, A.A.; Taz, M.; Lee, S.Y.; Lee, B.T. Enhancement of hemostatic property of plant-derived oxidized nanocellulose-silk fibroin-based scaffolds by thrombin loading. Carbohydrate Polymers 2019, 208, 168–179. DOI: 10.1016/j.carbpol.2018.12.056

[39] Li, S.; Bai, N.; Liu, X.; Mao, W.; Jin, L.; Fu, H.; Shou, Q. Fabricating oxidized cellulose sponge for hemorrhage control and wound healing. ACS Biomaterials Science and Engineering 2023. DOI: 10.1021/acsbiomaterials.3c00018

[40] Mohammed, I.H.; Hameed, A.T.; Salman, H.F. Phytochemical and biological of Anthemis nobilis (Asteraceae family) a native herb of Iraq. Systematic Reviews in Pharmacy 2020, 11(2), 458–461.

[41] SUNASEE, Rajesh; HEMRAZ, Usha D.; CKLESS, Karina. Cellulose nanocrystals: A versatile nanoplatform for emerging biomedical applications. Expert opinion on drug delivery, 2016, 13.9: 1243-1256.

[42] Shankaran, D. R. (2018). Cellulose nanocrystals for health care applications. In Applications of nanomaterials (pp. 415-459). Woodhead Publishing.

[43] Warkentin, T.E., 2014. Anticoagulant failure in coagulopathic patients: PTT confounding and other pitfalls. Expert opinion on drug safety, 13(1), pp.25-43.

[44] Palta, S., Saroa, R., and Palta, A. (2014). Overview of the coagulation system. Indian journal of anaesthesia, 58(5), 515-523.

[45] Mikaelsson, M. E. (1991, September). The role of calcium in coagulation and anticoagulation. In Coagulation and Blood Transfusion: Proceedings of the Fifteenth Annual Symposium on Blood Transfusion, Groningen 1990, organized by the Red Cross Blood Bank Groningen-Drenthe (pp. 29-37). Boston, MA: Springer US.

[46] Saikia, D., Wiley, J., Bhatia, S., and Roy, I. (2018). Silica nanoparticle–endothelial interaction: Uptake and effect on platelet adhesion under flow conditions. ACS Applied Bio Materials, 1(3), 864–872.

[47] Mosesson, M. W. (2005). Structure and functions of fibrinogen and fibrin. In Progress in Molecular Biology and Translational Science (Vol. 128, pp. 1–41).

[48] Pavan, C., Zivanovic, S., Mikulic, M., Tran, H. T., and Hristozov, D. (2023). Physico-chemical approaches to investigate surface hydroxyls as determinants of molecular initiating events in oxide particle toxicity. International Journal of Molecular Sciences, 24(14), 11482. 8 (2024).